Journal of Chromatography A 1687 (2023) 463655

Contents lists available at ScienceDirect

Journal of Chromatography A

journal homepage: www.elsevier.com/locate/chroma

Parameter-by-parameter method for steric mass action model of ion exchange chromatography: Simplified estimation for steric shielding factor

Yu-Cheng Chen, Shan-Jing Yao, Dong-Qiang Lin*

Zhejiang Key Laboratory of Smart Biomaterials, Key Laboratory of Biomass Chemical Engineering of Ministry of Education, College of Chemical and Biological Engineering, Zhejiang University, Hangzhou 310027, China

ARTICLE INFO

Article history:
Received 26 September 2022
Revised 16 November 2022
Accepted 16 November 2022
Available online 17 November 2022

Keywords:
Ion-exchange chromatography
Steric mass action model
Model calibration
Steric shielding factor

ABSTRACT

Mechanistic models play a crucial role in the process development and optimization of ion-exchange chromatography (IEC). Recent researches in steric mass action (SMA) model have heightened the need for better estimation of nonlinear parameter, steric shielding factor σ. In this work, a straightforward approach combination of simplified linear approximation (SLA) and inverse method (IM) was proposed to initialize and further determine σ, respectively. An existed, unique, and positive σ can be derived from SLA. Compared with linear approximation (LA) developed in our previous study, σ of the multi-component system can be calculated easily without solving the complex system of linear equations, leading to a time complexity reduction from $O(n^3)$ to $O(n)$. The proposed method was verified first in numerical experiments about the separation of three charge variants. The calculated σ was more reasonable than that of LA, and the error of elution profiles with the parameters estimated by SLA+IM was only one-sixth of that by LA in numerical experiments. Moreover, the error accumulation effect could also be reduced. The proposed method was further confirmed in real-world experiments about the separation of monomer-dimer mixtures of monoclonal antibody. The results gave a lower error and better physical understanding compared to LA. In conclusion, SLA+IM developed in the present work provides a novel and straightforward way to determine σ. This simplification would help to save the effort of calibration experiments and accelerate the process development for the multi-component IEC separation.

1. Introduction

Computer-aided process development shows promising applications in the downstream processing of biopharmaceuticals [1,2]. These approaches are capable of saving lots of materials, manpower, and costs compared to the traditional trial-and-error methods [3]. For protein separation with ion-exchange chromatography (IEC), mechanistic models are becoming preferable and popular because of their in-depth physical interpretation and excellent interpolation [4–6].

The essential core of IEC process modeling is the isotherm model [6]. The stoichiometric displacement model (SDM) based on the law of mass action is one of the most popular isotherm models [7]. However, this model can only be used under diluted conditions [8]. To better describe the isotherm, a nonlinear parameter named shielding factor σ was introduced by Brooks and Cramer [9] who considered the steric hindrance of bound protein on the salt counter-ion binding. This well-established modification was named as steric mass action (SMA) model, which can account for both the salt dependence of protein adsorption and the steric hindrance under nonlinear conditions [10]. The magnitude of σ is dominated by the size exclusion effects and molecular weight [11]. In addition to steric hindrance, σ is affected by the lateral protein-protein interaction at high loadings [12], as well as the repulsive effect caused by ligand-protein interactions [13]. In general, σ is important for the SMA model. However, its estimation is a challenging task [14].

Batch adsorption experiments are the most direct and frequent method to estimate σ, but this off-column method is a labor-intensive and cumbersome procedure that requires adequate quantities of pure target protein and impurities [15]. At high loadings or under overload conditions, estimating σ of individual specie separately cannot be transplanted into the complex multi-component system because σ is an interactive parameter that will change with the existence of other proteins. On the contrary, column experiments are able to reduce calibration experimental efforts, which can be classified into two groups: breakthrough experi-

* Corresponding author.
E-mail address: lindq@zju.edu.cn (D.-Q. Lin).

https://doi.org/10.1016/j.chroma.2022.463655
0021-9673/

ments [9,14,16,17], and linear gradient elution experiments (LGEs) [18,19]. Osberghaus et al. [14] investigated two breakthrough experiment strategies for estimating σ, and found that the numerous pure components were required still. Conversely, Rischawy et al. [20] used the inverse method (IM) to obtain σ by LGE profiles at high loadings in a multi-component system, and it was found that fewer experiments were required compared to the breakthrough experiment method. IM is a time-consuming iterative procedure including heuristic algorithm for researching the initial guess and deterministic algorithm for figuring out the determined value [21]. Another significant limitation of IM is the inability to avoid multiple solutions of σ. Thus, it is difficult to obtain a physically meaningful result [22].

To solve the above problems, the parameter-by-parameter (PbP) method was developed by our group [19] from a SMA model-based retention model. The PbP method consists of four steps, where four SMA parameters with in-depth physical understanding can be estimated one-at-a-time. σ can be calibrated in the third step named as the linear approximation (LA), which is significantly different from the above literature methods. Without any iteration, including heuristic and deterministic algorithms, a reasonable and physically meaningful σ can be obtained directly based on several LGE profiles. However, it was observed that the use of LA is limited by many conditions and cannot provide a one-size-fits-all solution. Firstly, it is necessary to solve a complex system of linear equations. Sometimes it is in multi-component systems that the linear system has no solution, leading to the failure of LA. Secondly, even though the linear system has solution, the computational effort of obtaining the coefficient matrix and solving the linear system increases steeply for the multi-component system. Thirdly, it is critical that LA cannot provide a positive and reasonable shielding factor sometimes. In fact, σ that accounts for the number of binding sites on the adsorbent surface shielded by steric mass action should be positive [9,17]. The unacceptable results may be because the loadings of calibration experiments are beyond the establishment scope of LA. A promising solution is to introduce IM for further improvement, which means σ would be initialized first and then determined by IM. Similar approaches have been reported to determine isotherm parameters. For example, Saleh et al. [18] developed a straightforward approach to calculate the initial guess of linear SMA parameters that was regarded as the input of IM. The likely method has been modified by Shekhawat et al. [15] for estimating the initial inputs of extended Langmuir isotherm parameters. Therefore, a better choice is to develop a new method which is valid for the multi-component system.

Based on the above analysis, a simplified linear approximation (SLA) coupled with IM would be developed in this work. σ would be initialized by SLA without solving any linear system and further estimated by IM, named as SLA+IM. In our previous work, it was found that there were some special elements in the coefficient matrix of LA linear system, which could be neglected in ideal situations. Based on this assumption, the LA coefficient matrix would be simplified to a diagonal matrix of SLA, which means SLA can be easily calculated. Then, the reasonable and physically meaning σ determined by SLA would be verified from the view of mathematics. To evaluate the feasibility and effectiveness of SLA+IM, a series of numerical experiments about three charge variants as well as real-world experiments about the separation of monomer-dimer mixtures of monoclonal antibodies (mAbs) would be conducted.

2. Materials and methods

2.1. Mechanistic model

The detailed description of the mechanistic model used in this work can be found in our previous study [19]. Here, only a necessary overview is highlighted.

2.1.1. Equilibrium dispersive model

The equilibrium dispersive model (EDM) is given by:

$$\frac{\partial c_i}{\partial t}(z,t) = -\frac{u}{\varepsilon_t}\frac{\partial c_i}{\partial z}(z,t) + D_{app}\frac{\partial^2 c_i}{\partial z^2}(z,t) - \frac{1-\varepsilon_t}{\varepsilon_t}\frac{\partial q_i}{\partial t}(z,t) \quad (1)$$

where c_i and q_i denote the mobile-phase and stationery-phase concentration of component i (mol/L), respectively. u represents the superficial velocity of liquid phase (m/s). ε_t indicates the total porosity. z and t are the axial position (m) and time (s), respectively. D_{app} is the apparent axial dispersion coefficient (m^2/s).

Initial conditions:

$$c_{inj,i}(t_{inj}) = \begin{cases} c_{inj}x_i & 0 < t \le t_{inj} \\ 0 & t > t_{inj} \end{cases} \quad (2)$$

where c_{inj} and t_{inj} are the injection concentration (mol/L) and time (s), respectively. $c_{inj,i}$ and x_i are the injection concentration (mol/L) and the mole fraction of protein i, respectively.

Boundary conditions:

$$D_{app}\frac{\partial c_i}{\partial z}(0,t) = \frac{u}{\varepsilon_t}\left[c_i(0,t) - c_{inj,i}(t)\right] \quad (3)$$

$$D_{app}\frac{\partial c_i}{\partial z}(L,t) = 0 \quad (4)$$

where L represents column length (m).

2.1.2. Steric mass action model

The kinetic SMA model is given by:

$$k_{kin,i}\cdot\frac{\partial q_i}{\partial t}(z,t) = k_{eq,i}\left[\Lambda - \sum_{j=1}^{n}\left(\nu_j+\sigma_j\right)\cdot q_j(z,t)\right]^{\nu_i}\cdot c_i(z,t) - q_i(z,t)\cdot c_s^{\nu_i}(z,t) \quad (5)$$

$$q_s(z,t) = \Lambda - \sum_{j=1}^{n}\nu_j\cdot q_j(z,t) \quad (6)$$

where $k_{kin,i}$, $k_{eq,i}$, ν_i, and σ_i are the kinetic coefficient, equilibrium coefficient, characteristic charge, and shielding factor of protein i, respectively. Λ represents the total ion-exchange capacity for binding (mol/L). c_s and q_s are the mobile-phase and stationery-phase concentration of salt (mol/L), respectively. n is the total number of components.

To solve the above mechanistic model, an efficient numerical method named the discontinuous Galerkin finite element method [23,24] was implemented by Python 3.10 with the open source tools, including NumPy [25], SciPy [26], scikit-opt, and Matplotlib [27].

2.2. Model calibration

Firstly, ν and k_{eq} are estimated by first linear regression (LR1) and second linear regression (LR2) of the PbP method proposed in the previous work [19], respectively. Then, SLA developed in this work is used to determine the initial guess of σ for replacement of LA. Finally, the initialized σ and k_{kin} initialized by the traditional heuristic algorithm, would be applied as the input of deterministic algorithm for further estimation. The new PbP method coupled with SLA is shown in Fig. 1.

2.3. Numerical experiment

A series of numerical experiments with three charge variants were conducted. All parameters of column geometry, operating conditions, and mass transport, as well as the loading, eluting, and washing phases were consistent with our previous study [19].

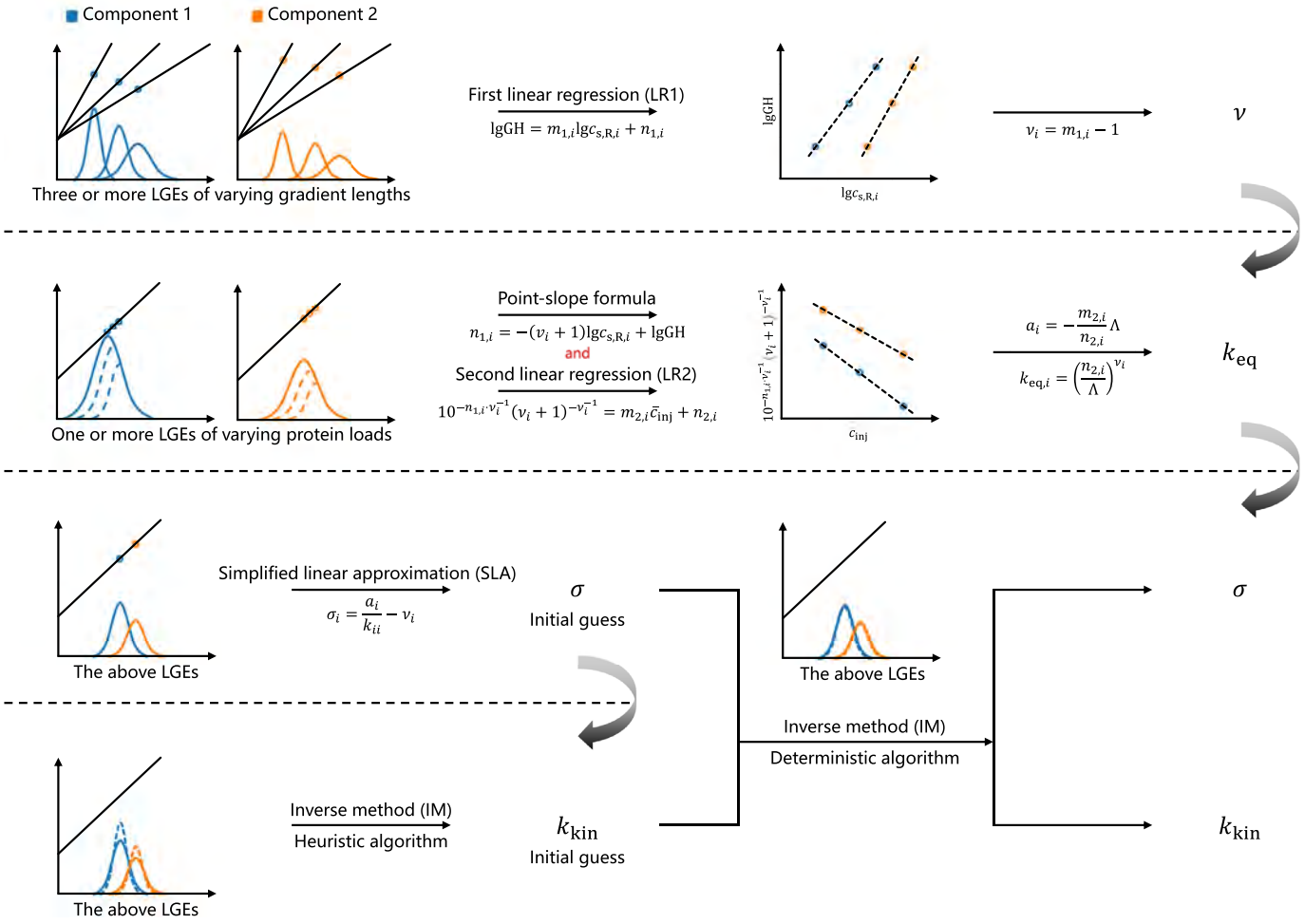

Fig. 1. Scheme of parameter-by-parameter method coupled with SLA. LGEs: linear gradient elution experiments.

Table 1
Binding parameters of proteins estimated by different methods in numerical experiments.

Parameter	Unit	Set values	LA	SLA+IM
ν	–	[6.00, 7.00, 8.00]	[6.01, 7.06, 8.07]	
k_{eq}	–	[0.100, 0.200, 0.400]	[0.092, 0.180, 0.363]	
σ	–	[51.0, 50.0, 49.0]	[133.5, 88.8, 65.6]	[44.7, 43.1, 38.5]
k_{kin}	sM^{ν}	[0.100, 0.100, 0.100]	[0.176, 0.118, 0.086]	[0.100, 0.097, 0.101]
L^2-error	–	–	0.344	0.059

The binding parameters of proteins have been modified as demonstrated in Table 1. There are six LGEs in this study, including three in different gradient lengths for fitting to LR1 and another three at different loadings for fitting to LR2.

The ratio of the injected amount $\bar{c}_{inj} = c_{inj} \cdot u \cdot t_{inj}/L$ to the saturated adsorption capacity q_{max} is defined as the loading factor as:

$$LF = \frac{\bar{c}_{inj}}{q_{max}}. \tag{7}$$

For multi-component systems with the SMA model, it is assumed that x_i, $q_{max,j}$, and the sum of ν and σ of individual components are identical based on a monomeric assumption [20,28]. Then, LF can be derived as:

$$\begin{aligned} LF &= \frac{\bar{c}_{inj}}{nq_{max,j}} = \frac{\nu+\sigma}{nq_{max,j}(\nu+\sigma)}\bar{c}_{inj} \\ &= \frac{\nu+\sigma}{\sum_{j=1}^{n}(\nu_j+\sigma_j)q_{max,j}}\bar{c}_{inj} = \frac{\nu+\sigma}{\Lambda}\bar{c}_{inj} \end{aligned} \tag{8}$$

where note that in numerical experiments $LF_{col} = LF/\varepsilon_t$ is employed.

2.4. Real-world experiments

The real-world experimental data from Reck et al. [29] and Creasy et al. [30] used in our previous paper [19] about the separation of mAb monomer-dimer mixtures were also applied in this work.

3. Results and discussion

3.1. Development of simplified linear approximation

To estimate σ by LA in our previous work [19], it is assumed that the coefficient matrix **K** is invertible and positive-definite so that the below linear system can be solved. In fact, **K** is not always

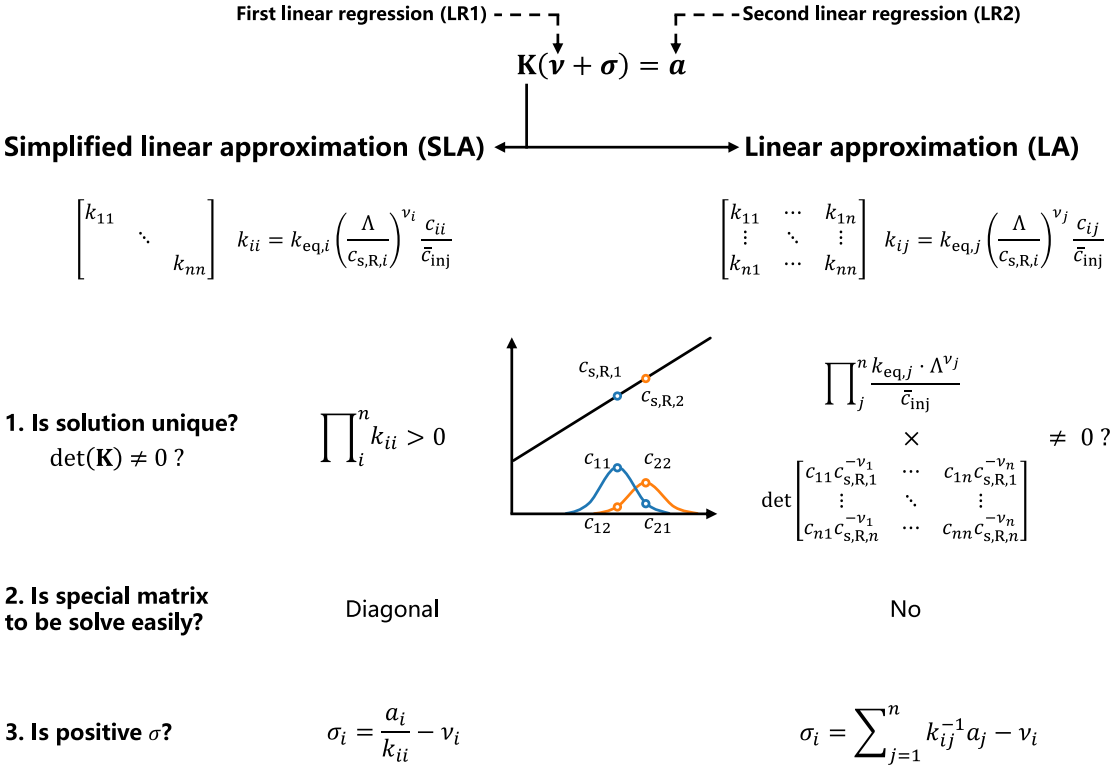

Fig. 2. A comparison between SLA and LA for estimating σ in three aspects.

positive-definite, in which the linear system cannot be solved.

$$\begin{bmatrix} k_{11} & \cdots & k_{1n} \\ \vdots & \ddots & \vdots \\ k_{n1} & \cdots & k_{nn} \end{bmatrix}\begin{bmatrix} \nu_1+\sigma_1 \\ \vdots \\ \nu_n+\sigma_n \end{bmatrix}=\begin{bmatrix} a_1 \\ \vdots \\ a_n \end{bmatrix}. \tag{9}$$

The necessary and sufficient condition to ensure the existence of solution of Eq. (9) is the nonzero determinant of $\mathbf{K}$ ($\det(\mathbf{K})\neq 0$), which can be derived using $k_{ij}=k_{\mathrm{eq},j}\cdot(\frac{\Lambda}{c_{\mathrm{s,R},i}})^{\nu_j}\cdot\frac{c_{ij}}{\bar{c}_{\mathrm{inj}}}$ as:

$$\det(\mathrm{K})=\prod_j^n\frac{k_{\mathrm{eq},j}\cdot\Lambda^{\nu_j}}{\bar{c}_{\mathrm{inj}}}\cdot\det\begin{bmatrix} c_{11}c_{\mathrm{s,R},1}^{-\nu_1} & \cdots & c_{1n}c_{\mathrm{s,R},1}^{-\nu_n} \\ \vdots & \ddots & \vdots \\ c_{n1}c_{\mathrm{s,R},n}^{-\nu_1} & \cdots & c_{nn}c_{\mathrm{s,R},n}^{-\nu_n} \end{bmatrix} \tag{10}$$

where c_{ij} and $c_{\mathrm{s,R},i}$ represent the mobile-phase concentration of component j and salt concentration at the retention time of protein i, respectively. To our knowledge, the first term $\prod_j^n\frac{k_{\mathrm{eq},j}\cdot\Lambda^{\nu_j}}{\bar{c}_{\mathrm{inj}}}>0$, but the second term is not always nonzero. That is to say, it is questionable whether the LA solution exists. Moreover, although the LA linear system has a unique solution, it is still cumbersome to solve owing to the common shape of $\mathbf{K}$, especially when the number of components increases for the complex separation system.

In addition, all calculated σ should be positive as previously stated. Given the element k_{ij}^{-1} in $\mathbf{K}^{-1}$ and using Eq. (9), the below formula can be obtained as:

$$\sigma_i=\sum_{j=1}^n k_{ij}^{-1}a_j-\nu_i>0. \tag{11}$$

For the complex multi-component separation system, it is hard to utilize Eq. (11) as a preliminary analysis of the signature of σ. To ensure σ positive, many Eq. (11) should be satisfied, and the number of equations is equal to the number of components. Based on our previous work, sometimes σ of partial proteins estimated by LA were negative unexpectedly. In this situation, the above constraint conditions could not be valid, which runs counter to the physical understanding of σ.

To address the above problems, LA was simplified to SLA. Under the assumption that the concentrations of other proteins c_{ij} ($i\neq j$) at the retention time of protein i tend to zero, k_{ij} can be reduced as:

$$k_{ii}=k_{\mathrm{eq},i}\cdot\left(\frac{\Lambda}{c_{\mathrm{s,R},i}}\right)^{\nu_i}\cdot\frac{c_{ii}}{\bar{c}_{\mathrm{inj}}}. \tag{12}$$

Therefore, $\mathbf{K}$ can be rewritten as:

$$\begin{bmatrix} k_{11} & & \\ & \ddots & \\ & & k_{nn} \end{bmatrix}. \tag{13}$$

The shape of $\mathbf{K}$ leads to a diagonal linear system. $\det(\mathbf{K})=\prod_i^n k_{ii}>0$ is always established so $\mathbf{K}$ is positive-definite. Thereby the linear system has a unique solution and can be easily calculated as:

$$\sigma_i=\frac{a_i}{k_{ii}}-\nu_i=\frac{a_i}{k_{\mathrm{eq},i}}\frac{\bar{c}_{\mathrm{inj}}}{c_{ii}}\left(\frac{c_{\mathrm{s,R},i}}{\Lambda}\right)^{\nu_i}-\nu_i. \tag{14}$$

It is a simple formula and provides an alternative way to estimate σ without solving the complex linear system and to keep σ greater than zero. Notably, SLA is equivalent to LA for the single-component system because there is only one element in $\mathbf{K}$. The comparison between SLA and LA is shown in Fig. 2.

In computer science, the time complexity of algorithm is a good way to measure the efficiency of algorithm. For a mixture system with n components using Gauss elimination method that is a classical method, and the time complexity of obtaining k_{ij} and solving Eq. (9) of LA are $O(n^2)$ and $O(n^3)$, respectively. Thereby the total time complexity of LA is $O(n^3)$, which equals the time complexity

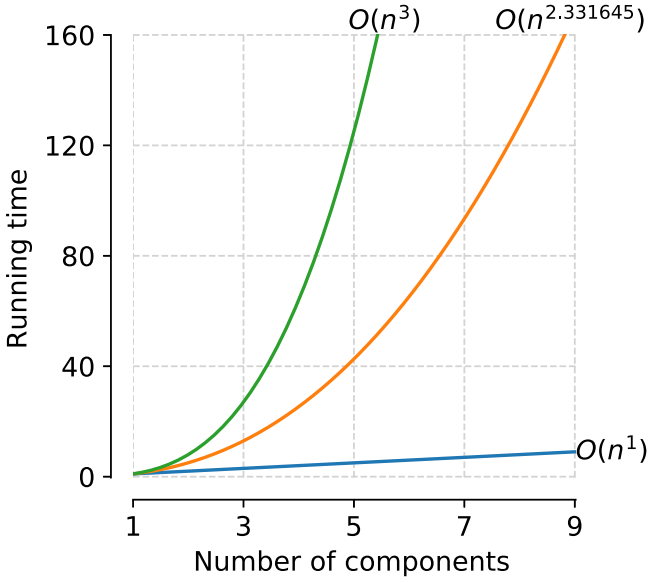

Fig. 3. Time complexity of different methods for estimating σ. $O(n^3)$: LA solved by Gauss elimination method, $O(n^{2.331645})$: LA solved by Peng and Vempala [31] method, and $O(n)$: SLA by straightforward calculation.

of solving the linear system. To our knowledge, the fastest method to solve the linear system in the world was developed by Peng and Vempala [31] with $O(n^{2.331645})$. However, the time complexity of calculating Eq. (14) of SLA is only $O(n)$, which means the running time would increase linearly with the growth of n. Here, aiming at the estimation of σ, the time complexity reduces to $O(n)$ without solving any linear system. The time complexity of the above methods can be compared in Fig. 3. In practical, the most common situation is that a chromatographic consists of at least three components, in which SLA is 27 times faster than LA with Gauss elimination method to calculate σ.

3.2. Numerical experiments

The proposed SLA method is validated in numerical experiments. Here, three-component numerical experiments were designed. All components in the chromatographic separation can be divided into three groups based on to their adsorptivity: weakly adsorbed component, target product, and strongly adsorbed component [32], which are also known as acidic, main, basic variants in cation exchange chromatography. Therefore, three species are simulated in numerical experiments for simplicity. Regarding the SMA model parameters, it is commonly thought that charge variants have significantly different ν and k_{eq} affecting the retention time owing to their intrinsic physicochemical properties, while their σ are similar because of similar molecular weights [11,20,28,33]. To satisfy the calculation of Eq. (8) as previously explained, a relationship between ν and σ was considered as $\nu_{\text{Acidic}} + \sigma_{\text{Acidic}} = \nu_{\text{Main}} + \sigma_{\text{Main}} = \nu_{\text{Basic}} + \sigma_{\text{Basic}}$, resulting in the values of σ as listed in Table 1. k_{kin} of all variants are kept identical because the method presented in this work was developed from the retention model that is not disturbed by k_{kin}. All calculations about the retention time are carried out by the moment analysis [34], including $c_{s,R}$, c_{ij}, and k_{ij}.

3.2.1. Estimation of characteristic charge and equilibrium coefficient

As published in the previous paper, LR1 is calculated by $c_{s,R}$ and GH of the elution profiles in different gradient lengths, as shown in Fig. 4a. The correlation coefficients of all variants are approximately 1.00. Afterwards, ν of all three components can be figured out as listed in Table 1.

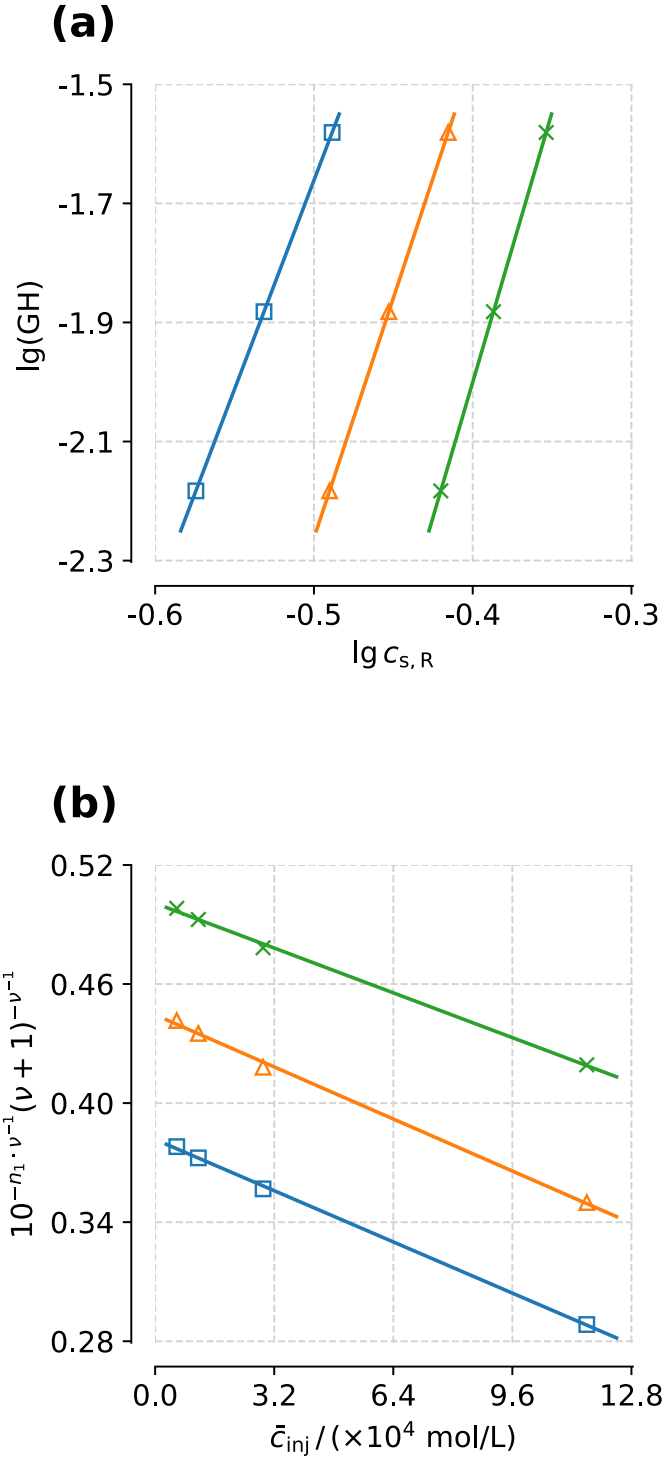

Fig. 4. First linear regression (a) and second linear regression (b) of numerical experiments. □: Acidic, △: Main, ×: Basic variants.

The above estimated ν are used to measure the intercepts of three LGEs at varying loadings by the point-slope formula. Then, LR2 can be figured out by the above ν and intercepts as shown in Fig. 4b. Significant positive correlations are found between $10^{-n_{1,i}\cdot\nu_i^{-1}}(\nu_i+1)^{-\nu_i^{-1}}$ and $\bar{c}_{\text{inj}}$ for all variants. The high R^2 indicates that LR2 of the PbP method can work well for the multi-component experiment. Then the slopes and intercepts of LR2 can be applied to determine a and k_{eq}, and the results are listed in Table 1.

$$\mathbf{K} \times \boldsymbol{\nu}+\boldsymbol{\sigma} = \boldsymbol{a}$$

$$\begin{bmatrix} 0.782 & 0.086 & 0.002 \\ 0.001 & 0.820 & 0.104 \\ 0.000 & 0.004 & 0.846 \end{bmatrix} \times \begin{bmatrix} 0.842 & 0.094 & 0.003 \\ 0.001 & 0.881 & 0.112 \\ 0.000 & 0.002 & 0.879 \end{bmatrix} \times \begin{bmatrix} 0.986 & 0.281 & 0.031 \\ 0.006 & 0.978 & 0.296 \\ 0.000 & 0.013 & 0.882 \end{bmatrix} \times \begin{bmatrix} 1.870 & 2.650 & 3.243 \\ 0.081 & 1.505 & 1.769 \\ 0.000 & 0.114 & 1.045 \end{bmatrix} \times \begin{bmatrix} \nu_{\mathrm{Acidic}}+\sigma_{\mathrm{Acidic}} \\ \nu_{\mathrm{Main}}+\sigma_{\mathrm{Main}} \\ \nu_{\mathrm{Basic}}+\sigma_{\mathrm{Basic}} \end{bmatrix} = \begin{bmatrix} a_{\mathrm{Acidic}} \\ a_{\mathrm{Main}} \\ a_{\mathrm{Basic}} \end{bmatrix}$$

Fig. 5. Coefficient matrix **K** with LF_{col} of 1%, 2%, 5%, and 10% from top to bottom of numerical experiments. Black in **K**: k_{ij} $(i = j)$ for SLA of PbP method; gray in **K**: additional k_{ij} $(i \neq j)$ for LA of PbP method.

3.2.2. Estimation of shielding factor and kinetic coefficient

(1) LA for shielding factor

For comparison, the LA calculation is performed firstly. An exactly computed **K** that consists of the black $(i = j)$ and gray $(i \neq j)$ elements is shown in Fig. 5. It can be found that all elements in **K** are nonzero and they should be calculated exactly. Moreover, **K** has no distinguishing feature in shape, like an upper/lower triangular or diagonal matrix. Therefore, the linear system cannot be easily resolved. The computational effort of obtaining all elements in **K** and solving the linear system surges steeply when the number of components increases. Although the above analysis raises the question whether the LA linear system has a unique solution, it can still be solved in this case.

σ can be obtained after solving the linear system of all four calibration experiments with great effort. An unexcepted result with negative σ would be found at 10% LF_{col}, which should be positive according to previous analysis. So, this result is excluded from the calculation of mean σ, leading to σ_{Acidic} =133.5, σ_{Main} =88.8, and σ_{Basic} =65.6. Although the quantitative association of estimated σ of three variants is established, all of them are greater than the ground truths (σ_{Acidic} =51.0, σ_{Main} =50.0, and σ_{Basic} =49.0), especially for the acidic variant. It is obvious that the error of σ_{Acidic} is unacceptable. The undesirable outcomes could be attributed to the restrictive conditions of using LA. In general, these strict conditions may hinder the application and generalization of the PbP method coupled with LA.

k_{kin} is then estimated by IM with elution profiles, whose initial guesses range from 1.0E-06 to 10.0 for all three variants. The objective function of the optimization problem is defined as:

$$\min_{k_{\mathrm{kin}}} J(c_h; k_{\mathrm{kin}}) : \min_{k_{\mathrm{kin}}} \sum_{j=1}^{m}\sum_{i=1}^{n} \frac{\|c_i - c_{h,i}(z,t;k_{\mathrm{kin},i})\|_{L^2}^2}{\|c_i\|_{L^2}^2} \tag{15}$$

where m is the total number of LGEs.

After solving the optimization problem with three hundred evaluations (200 for the heuristic algorithm and 100 for the deterministic algorithm), k_{kin} of acidic, main, and basic variant are obtained as 0.176, 0.118, and 0.086, respectively. It can be seen that the error of $k_{\mathrm{kin,acidic}}$ is unanticipatedly high. This disparity may be due to the error accumulation effect (the unreasonable σ_{Acidic}), which means the error of former step would accumulate to the latter one because all parameters are determined in sequence for the PbP method.

Using the above estimated SMA model parameters, the elution curves can be simulated as shown in Fig. 6. The agreement between experiments and model simulations is calculated by L^2-error, which is 0.334 in this case. A remarkable difference can be found in that the simulated peak heights of all three variants are obviously lower than those of experiments (solid lines) under all six conditions. For the kinetic SMA formalism used in the present work, the peak height of individual component is dominated by σ and k_{kin} [35]. A lower simulated peak indicates that the calibrated k_{kin} or σ are unrealistically higher than the ground truths. Furthermore, this unreality of k_{kin} may be caused by the undesirable σ considering the error accumulation effect. It should be noted that the agreement becomes worse with the increase of loading, which is mainly attributed to the unreasonable nonlinear parameter σ.

To enhance the fitting degree of elution curves and reduce L^2-error, it is worthwhile to consider the value of σ with LA as the initial guess for IM rather than the determined value. Obviously, it is not necessary to compute the initial guess exactly by solving the complex linear system as mentioned above. Therefore, a straightforward method named as SLA was developed to determine the initial guess of σ.

(2) SLA+IM for shielding factor

Different from the above method based on LA, σ in this part would be initialized by SLA and further estimated by IM. Initial guesses of k_{kin} were also determined by the heuristic algorithm after 200 iterations with the range from 1.0E-06 to 10.0. The objective function is rewritten as:

$$\min_{k_{\mathrm{kin}},\sigma} J(c_{h,i}; k_{\mathrm{kin}}, \sigma) : \min_{k_{\mathrm{kin}},\sigma} \sum_{j=1}^{m}\sum_{i=1}^{n} \frac{\|c_i - c_{h,i}(z,t;k_{\mathrm{kin},i},\sigma_i)\|_{L^2}^2}{\|c_i\|_{L^2}^2}. \tag{16}$$

The optimal σ and k_{kin} would be found by solving the above optimization problem using the deterministic algorithm after 100 iterations with elution profiles simultaneously as shown in Fig. 1.

K of SLA calculated by Eq. (12) is shown as the black ones in Fig. 5, which are much greater than those of LA (gray ones in Fig. 5) in the same row. The results are logical and support the previous assumption on the derivation of SLA in Eq. (12), under which k_{ij} of LA $(i \neq j$, gray one in Fig. 5) is small enough to be neglectable and the computational effort of **K** can be reduced, especially for the multi-component system. Owing to the diagonal shape of **K**, σ can be directly estimated by Eq. (14) and a of LR2 without solving the complex linear system of Eq. (9). The mean shielding factors are σ_{Acidic} =120.9, σ_{Main} =106.2, and σ_{Basic} =88.5.

It is interesting to find that the quantitative relationship of σ of three variants is still established due to the reasonable derivation of SLA, but all of them are greater than ground truths. The results indicate that all σ determined by SLA close to those produced by LA. Most importantly, the recalibrated σ are positive compared to LA in all six conditions, which is in accordance with its physical interpretation.

The above comparison between SLA and LA reveals that there is no significant difference between these two methods for the estimation of σ if considering SLA as an approximation and simplification of LA and using the SLA output as the input of deterministic algorithm. However, the computational procedure, the strict conditions, and the sign of solution are strikingly distinct. As an appropriate simplification of LA, the SLA result may not be accurate enough to be a determined value of the SMA model. It is worthwhile to have the SLA output as the input of the deterministic algorithm to further enhance it. After that, four estimated parameters are obtained finally as listed in Table 1.

For the parameter σ, σ_{Acidic}(44.7)> σ_{Main}(43.1)> σ_{Basic}(38.5). It means that σ estimated by SLA+IM can reproduce the tiny deviation of designed σ, σ_{Acidic}(51.0)> σ_{Main}(50.0)> σ_{Basic}(49.0). The SLA+IM results are closely related to the ground truths, which are more reasonable than the determined values estimated by LA.

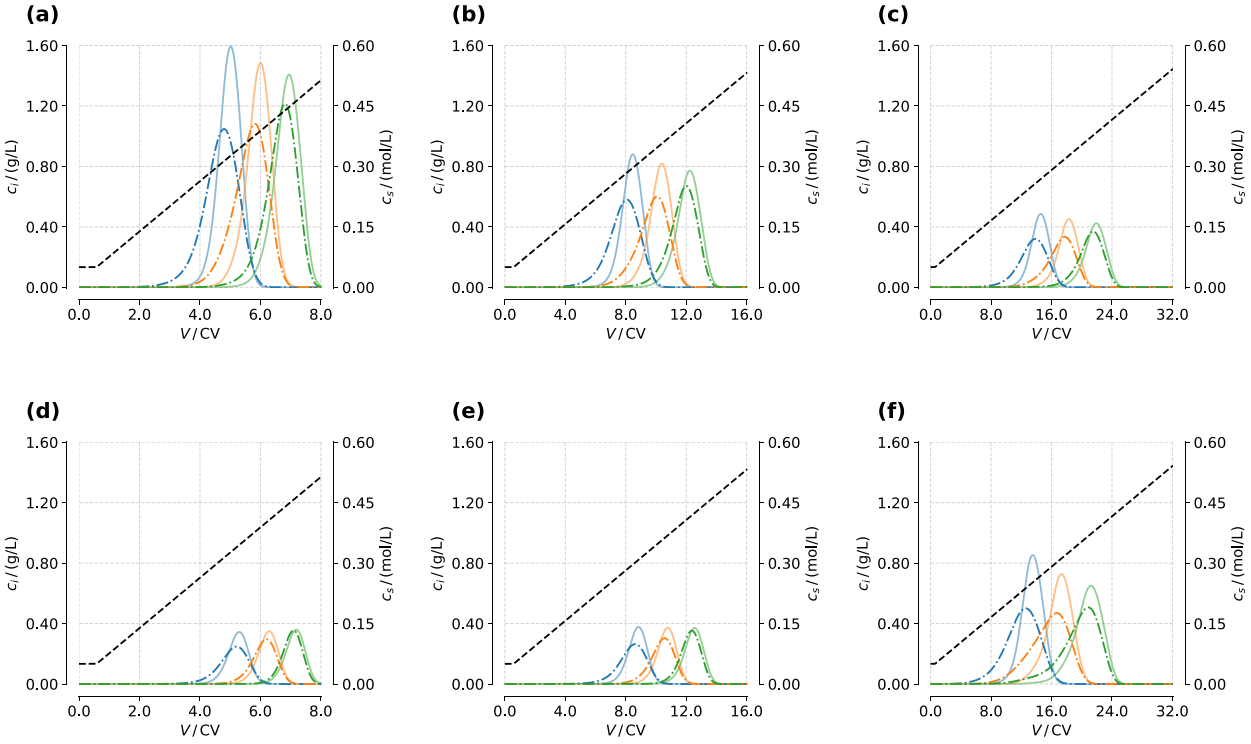

Fig. 6. Linear gradient elution curves of numerical experiments (solid lines) and model simulation using PbP method coupled with LA (dotted-dashed lines). Dashed lines: salt gradients at column outlet. (a) 5% LF_{col} and 8 CV gradient, (b) 5% LF_{col} and 16 CV gradient, (c) 5% LF_{col} and 32 CV gradient, (d) 1% LF_{col} and 8 CV gradient, (e) 2% LF_{col} and 16 CV gradient, (f) 10% LF_{col} and 32 CV gradient.

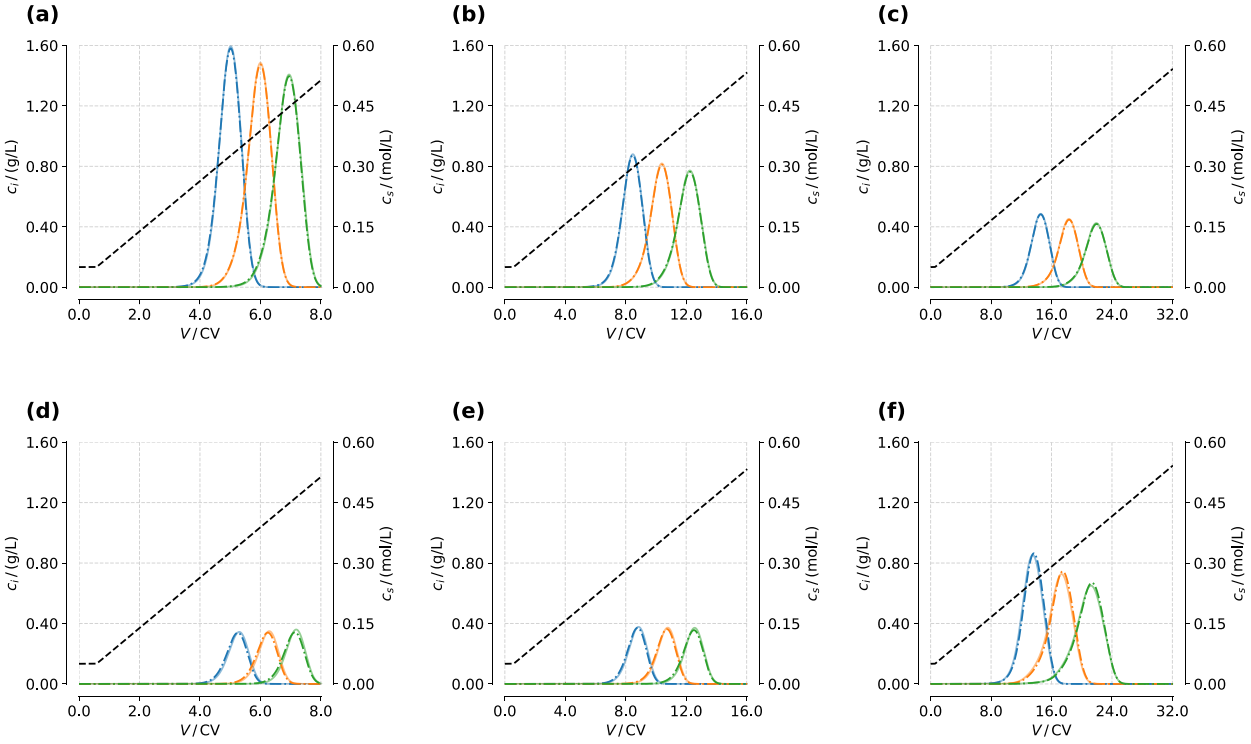

Fig. 7. Linear gradient elution curves of numerical experiments (solid lines) and model simulation using PbP method coupled with SLA+IM (dotted-dashed lines). Dashed lines: salt gradients at column outlet. (a) 5% LF_{col} and 8 CV gradient, (b) 5% LF_{col} and 16 CV gradient, (c) 5% LF_{col} and 32 CV gradient, (d) 1% LF_{col} and 8 CV gradient, (e) 2% LF_{col} and 16 CV gradient, (f) 10% LF_{col} and 32 CV gradient.

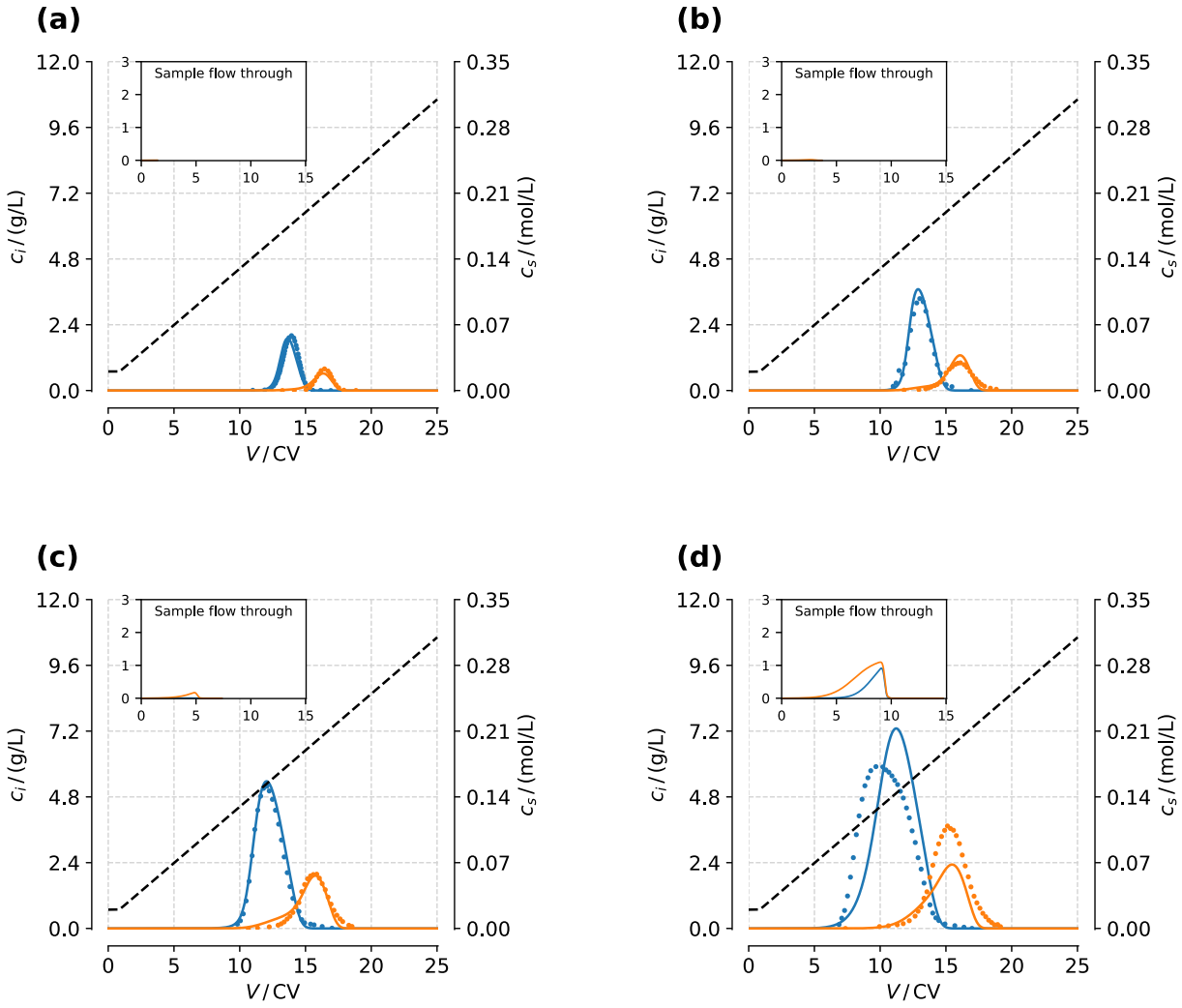

Fig. 8. Linear gradient elution curves of real-world experiments (solid lines) and model simulation using PbP method coupled with SLA+IM (dotted-dashed lines). Dashed lines: salt gradients at column outlet. Loadings: (a) 4, (b) 10, (c) 20 and (d) 40 g/L column. The subfigures at upper left corner show the sample flow through.

For the parameter k_{kin}, it could be found that the results almost converge to the ground truths due to the reasonable σ and the reduction of the error accumulation effect as previously discussed.

The elution curves simulated by the above calibrated parameters are shown in Fig. 7. SLA+IM achieves a satisfactory agreement with the L^2-error of 0.059 compared to LA (0.344). All the simulated elution profiles almost stack up with the experiments due to the rational parameter estimation. The simulated peak heights of all three variants are in agreement with the experiment (solid lines), which confirms the previous discussion that better estimation of σ and k_{kin} are very important and can significantly improve the fitting result.

3.3. Real-world experiments

The proposed method was challenged in real-world experiments on the separation of mAb monomer-dimer mixtures.

To justify the assumption of SLA in this real-world case, the full **K** of four LGEs for estimating σ were calculated firstly as:

$$\begin{bmatrix} 6.468 & 0.042 \\ 0.003 & 0.847 \end{bmatrix} \begin{bmatrix} 7.371 & 0.421 \\ 0.031 & 0.641 \end{bmatrix} \begin{bmatrix} 10.329 & 0.765 \\ 0.029 & 0.877 \end{bmatrix} \begin{bmatrix} 27.043 & 4.988 \\ 0.020 & 1.224 \end{bmatrix} \quad (17)$$

where the loading increases from 4 to 40 g/L column. The results verify the assumption that the diagonal element of **K** is much greater than other elements in the same row. Based on these diagonal elements, initial guesses of σ (σ_M =24.6 and σ_D =82.0) can be easily figured out by Eq. (14) without solving any linear system, which are applied as the input of IM for further estimation.

After solving the same optimization problem defined in Eq. (16) with initial guesses estimated by SLA, σ_M =22.9 and σ_D =45.9 are obtained. It is interesting to find that $\nu_M + \sigma_M$ is nearly one half of $\nu_D + \sigma_D$, which is in accordance with the physical interpretation of this nonlinear parameter [9,17]. It is commonly thought that steric hindrance is associated with size exclusion effects and molecular weight [11]. In this case, $M_{r,M}$ (150 kDa) is roughly one half of $M_{r,D}$ (300 kDa), which reflects the relationship between $\nu_M + \sigma_M$ and $\nu_D + \sigma_D$ because of the in-depth physical understanding and reasonable development of SLA. This two-fold relationship is the basic assumption of the self-association (SAS) isotherm, which is an extended SMA model with consideration of the dimerization of monomer protein [36, 37]. Compared with the results of LA (σ_M =30.4 and σ_D =62.3 published in [19]), the parameters determined by SLA+IM decrease by the same proportion.

Based on the ν and k_{eq} presented in our previous study [19] and the above estimated parameters (σ and k_{kin}), the elution

Table 2
L^2-error calculated by different methods in real-world experiments.

Loading (g/L column)	LA		SLA+IM	
	Monomer	Dimer	Monomer	Dimer
4	0.344	0.277	0.242	0.241
10	0.221	0.317	0.129	0.230
20	0.198	0.231	0.093	0.149
40	0.365	0.465	0.462	0.388

curves can be generated as shown in Fig. 8. The L^2-error is reduced from 0.314 (LA published in [19]) to 0.270 (SLA+IM). The nonignorable error could be found for the loading of 40 g/L column as shown in Fig. 8d and Table 2. In this panel, the total simulated integral area of dimer is greatly less than that of measurement, which means some proteins flow through the column and are lost during the injection phase as shown in Fig. 8d. The saturated adsorption capacity of the SMA model is characterized by ν and σ simultaneously. σ has a dominant effect because σ is generally several times higher than ν. The higher σ, the greater the excessive protein losses. So, lower σ with SLA+IM (σ_M =22.9 and σ_D =45.9) are more reasonable than those with LA (σ_M =30.4 and σ_D =62.3). The excessive protein loss phenomenon means the experiment in Fig. 8d was conducted under overloading conditions, which cannot be comprehensively characterized by the classical SMA model [29,38]. Therefore, the agreement becomes worse with the loading increases, and the modified SMA model may tackle this problem [36,39,40].

In summary, the SLA outcome regarded as the input of IM provides a new strategy to obtain the initial guess of σ. In this way, the cost for searching the initial guess of σ can be reduced without solving a complex linear system by programming as LA, which can accelerate the model calibration process. σ initialized by SLA can provide a comprehensive physical cognizance of model parameters and avoid the multiple solutions known as the ill-posed problem. Most importantly, the above method would give an existed, unique, and positive solution of σ. On the other hand, the modified optimization problem of SLA causes an increase in the number of parameters determined by IM compared to LA. Although the modification will improve the fitting degree, it may cause the overfitting problem [41], which means that the model is accurately calibrated but just for the calibration experiments.

4. Conclusion

A straightforward approach (SLA+IM) to determine σ of the SMA model was proposed in this work for the multi-component IEC separation. Based on the reasonable assumption, SLA was developed from LA of the PbP method in our previous study. It was confirmed that the SLA solution was always existed, unique and positive, and the diagonal shape of **K** of SLA made σ calculated easily without solving the complex linear system compared to LA, leading to a time complexity reduction from $O(n^3)$ to $O(n)$.

A series of numerical experiments about three charge variants was conducted to assess the performance of LA and SLA+IM. For both two approaches, the estimation of ν and k_{eq} are identical, which can be implemented by LR1 and LR2 of the PbP method, respectively. After calculating **K** and solving the complex linear system programmatically, LA returned a disappointing result that σ and k_{kin} were unrealistically higher than the ground truths. This unreality made the error of σ further accumulate to the next step for estimating k_{kin}. Additionally, a negative σ was found at high loadings, which contradicted with its physical cognizance. For SLA+IM, the initial guess of σ can be easily obtained without solving the complex linear system. The calculated σ was more reasonable than that with LA. The error of σ was only one-sixth of that of LA, so the error accumulation from σ to k_{kin} was reduced. Furthermore, SLA+IM was confirmed in real-world experiments about the separation of mAb monomer-dimer mixtures. The results showed that the proposed method can be easily applied in a real-world case with better physically meaningful model parameters. This simplification of the estimation σ would help to save the cost of calibration experiments and accelerate the process development of multi-component systems, which is certainly useful to generalize and popularize the PbP method. Further research will focus on the applications of new PbP method coupled with SLA+IM for the separation and purification of complex protein mixtures.

Declaration of Competing Interest

The authors declare that they have no known competing financial interests or personal relationships that could have appeared to influence the work reported in this paper.

CRediT authorship contribution statement

Yu-Cheng Chen: Conceptualization, Data curation, Formal analysis, Methodology, Software, Validation, Visualization, Writing – original draft, Writing – review & editing. **Shan-Jing Yao:** Writing – review & editing. **Dong-Qiang Lin:** Conceptualization, Funding acquisition, Resources, Supervision, Writing – review & editing.

Data Availability

Data will be made available on request.

Acknowledgments

This work was supported by the National Key R&D Program of China (2021YFE0113300) and National Natural Science Foundation of China (22078286).

References

[1] V. Hebbi, S. Roy, A.S. Rathore, A. Shukla, Modeling and prediction of excipient and pH drifts during ultrafiltration/diafiltration of monoclonal antibody biotherapeutic for high concentration formulations, Sep. Sci. Technol. 238 (2020) 116392, doi:10.1016/j.seppur.2019.116392.
[2] G. Thakur, A.S. Rathore, Modelling and optimization of single-pass tangential flow ultrafiltration for continuous manufacturing of monoclonal antibodies, Sep. Sci. Technol. 276 (3–4) (2021) 119341, doi:10.1016/j.seppur.2021.119341.
[3] B.K. Nfor, P. Verhaert, L.A.M. van der Wielen, J. Hubbuch, M. Ottens, Rational and systematic protein purification process development: the next generation, Trends Biotechnol 27 (12) (2009) 673–679, doi:10.1016/j.tibtech.2009.09.002.
[4] J.W. Kou, H.L. Xiang, Z. Zhang, J. Zhang, G.Q. Wang, K. Dai, P.P. Yang, W. Zhuang, H.J. Ying, J.L. Wu, Mass transfer process and separation mechanism of sulfuric acid and aluminum sulfate mixture based on IEC technology: modeling, Sep. Sci. Technol. 285 (2) (2022) 120168, doi:10.1016/j.seppur.2021.120168.
[5] L.Z. Qiao, Y.C. Du, K.F. Du, Grafting diethylaminoethyl dextran to macroporous cellulose microspheres: a protein anion exchanger of high capacity and fast uptake rate, Sep. Sci. Technol. 297 (1) (2022) 121434, doi:10.1016/j.seppur.2022.121434.
[6] J.G. Outram, S.J. Couperthwaite, W. Martens, G.J. Millar, Application of nonlinear regression analysis and statistical testing to equilibrium isotherms: building an Excel template and interpretation, Sep. Sci. Technol. 258 (2021) 118005, doi:10.1016/j.seppur.2020.118005.
[7] W. Kopaciewicz, M.A. Rounds, J. Fausnaugh, F.E. Regnier, Retention model for high-performance ion-exchange chromatography, J. Chromatogr. 266 (AUG) (1983) 3–21, doi:10.1016/s0021-9673(01)90875-1.
[8] M. Rudt, F. Gillet, S. Heege, J. Hitzler, B. Kalbfuss, B. Guelat, Combined Yamamoto approach for simultaneous estimation of adsorption isotherm and kinetic parameters in ion-exchange chromatography, J. Chromatogr. A 1413 (2015) 68–76, doi:10.1016/j.chroma.2015.08.025.
[9] C.A. Brooks, S.M. Cramer, Steric mass-action ion-exchange - displacement profiles and induced salt gradients, AIChE J. 38 (12) (1992) 1969–1978, doi:10.1002/aic.690381212.

[10] S.R. Gallant, A. Kundu, S.M. Cramer, Modeling nonlinear elution of proteins in ion-exchange chromatography, J. Chromatogr. A 702 (1–2) (1995) 125–142, doi:10.1016/0021-9673(94)00992-i.
[11] C.R. Bernau, R.C. Japel, J.W. Hubbers, S. Nolting, P. Opdensteinen, J.F. Buyel, Precision analysis for the determination of steric mass action parameters using eight tobacco host cell proteins, J. Chromatogr. A 1652 (2021) 462379, doi:10.1016/j.chroma.2021.462379.
[12] W.S. Xu, F.E. Regnier, Protein-protein interactions on weak-cation-exchange sorbent surfaces during chromatographic separations, J. Chromatogr. A 828 (1–2) (1998) 357–364, doi:10.1016/s0021-9673(98)00641-4.
[13] A. Ladiwala, K. Rege, C.M. Breneman, S.M. Cramer, A priori prediction of adsorption isotherm parameters and chromatographic behavior in ion-exchange systems, Proc. Natl. Acad. Sci. U.S.A. 102 (33) (2005) 11710–11715, doi:10.1073/pnas.0408769102.
[14] A. Osberghaus, S. Hepbildikler, S. Nath, M. Haindl, E. von Lieres, J. Hubbuch, Determination of parameters for the steric mass action model–a comparison between two approaches, J. Chromatogr. A 1233 (2012) 54–65, doi:10.1016/j.chroma.2012.02.004.
[15] L.K. Shekhawat, A. Tiwari, S. Yamamoto, A.S. Rathore, An accelerated approach for mechanistic model based prediction of linear gradient elution ion-exchange chromatography of proteins, J. Chromatogr. A (2022) 463423, doi:10.1016/j.chroma.2022.463423.
[16] T.C. Huuk, T. Hahn, A. Osberghaus, J. Hubbuch, Model-based integrated optimization and evaluation of a multi-step ion exchange chromatography, Sep. Sci. Technol. 136 (2014) 207–222, doi:10.1016/j.seppur.2014.09.012.
[17] J. Morgenstern, G. Wang, P. Baumann, J. Hubbuch, Model-based investigation on the mass transfer and adsorption mechanisms of mono-pegylated lysozyme in ion-exchange chromatography, Biotechnol. J. 12 (9) (2017) 1700268, doi:10.1002/biot.201700255.
[18] D. Saleh, G. Wang, B. Muller, F. Rischawy, S. Kluters, J. Studts, J. Hubbuch, Straightforward method for calibration of mechanistic cation exchange chromatography models for industrial applications, Biotechnol. Prog. 36 (4) (2020) 12, doi:10.1002/btpr.2984.
[19] Y.C. Chen, S.J. Yao, D.Q. Lin, Parameter-by-parameter method for steric mass action model of ion exchange chromatography: theoretical considerations and experimental verification, J. Chromatogr. A 1680 (2022) 463418, doi:10.1016/j.chroma.2022.463418.
[20] F. Rischawy, D. Saleh, T. Hahn, S. Oelmeier, J. Spitz, S. Kluters, Good modeling practice for industrial chromatography: mechanistic modeling of ion exchange chromatography of a bispecific antibody, Comput. Chem. Eng. 130 (3) (2019) 14, doi:10.1016/j.compchemeng.2019.106532.
[21] Y. Luo, H.L. Zhang, M.L. Su, Q.H. Tang, J. Xu, W.F. Yu, Effects of mobile phase composition on key parameters for the design of preparative chromatography separation of equol enantiomers, Sep. Sci. Technol. 288 (4) (2022) 120645, doi:10.1016/j.seppur.2022.120645.
[22] L.K. Shekhawat, A.S. Rathore, An overview of mechanistic modeling of liquid chromatography, Prep. Biochem. Biotechnol. 49 (6) (2019) 623–638, doi:10.1080/10826068.2019.1615504.
[23] K. Meyer, J.K. Huusom, J. Abildskov, High-order approximation of chromatographic models using a nodal discontinuous Galerkin approach, Comput. Chem. Eng. 109 (2018) 68–76, doi:10.1016/j.compchemeng.2017.10.023.
[24] K. Meyer, S. Leweke, E. von Lieres, J.K. Huusom, J. Abildskov, ChromaTech: a discontinuous Galerkin spectral element simulator for preparative liquid chromatography, Comput. Chem. Eng. 141 (2) (2020) 107012, doi:10.1016/j.compchemeng.2020.107012.
[25] S.v.d. Walt, S.C. Colbert, G. Varoquaux, The NumPy array: a structure for efficient numerical computation, Comput. Sci. Eng. 13 (2) (2011) 22–30, doi:10.1109/MCSE.2011.37.
[26] P. Virtanen, R. Gommers, T.E. Oliphant, M. Haberland, T. Reddy, D. Cournapeau, E. Burovski, P. Peterson, W. Weckesser, J. Bright, S.J. van der Walt, M. Brett, J. Wilson, K.J. Millman, N. Mayorov, A.R.J. Nelson, E. Jones, R. Kern, E. Larson, C.J. Carey, İ. Polat, Y. Feng, E.W. Moore, J. VanderPlas, D. Laxalde, J. Perktold, R. Cimrman, I. Henriksen, E.A. Quintero, C.R. Harris, A.M. Archibald, A.H. Ribeiro, F. Pedregosa, P. van Mulbregt, A. Vijaykumar, A.P. Bardelli, A. Rothberg, A. Hilboll, A. Kloeckner, A. Scopatz, A. Lee, A. Rokem, C.N. Woods, C. Fulton, C. Masson, C. Häggström, C. Fitzgerald, D.A. Nicholson, D.R. Hagen, D.V. Pasechnik, E. Olivetti, E. Martin, E. Wieser, F. Silva, F. Lenders, F. Wilhelm, G. Young, G.A. Price, G.-.L. Ingold, G.E. Allen, G.R. Lee, H. Audren, I. Probst, J.P. Dietrich, J. Silterra, J.T. Webber, J. Slavič, J. Nothman, J. Buchner, J. Kulick, J.L. Schönberger, J.V. de Miranda Cardoso, J. Reimer, J. Harrington, J.L.C. Rodríguez, J. Nunez-Iglesias, J. Kuczynski, K. Tritz, M. Thoma, M. Newville, M. Kümmerer, M. Bolingbroke, M. Tartre, M. Pak, N.J. Smith, N. Nowaczyk, N. Shebanov, O. Pavlyk, P.A. Brodtkorb, P. Lee, R.T. McGibbon, R. Feldbauer, S. Lewis, S. Tygier, S. Sievert, S. Vigna, S. Peterson, S. More, T. Pudlik, T. Oshima, T.J. Pingel, T.P. Robitaille, T. Spura, T.R. Jones, T. Cera, T. Leslie, T. Zito, T. Krauss, U. Upadhyay, Y.O. Halchenko, Y. Vázquez-Baeza, C. SciPy, SciPy 1.0: fundamental algorithms for scientific computing in Python, Nat. Methods 17 (3) (2020) 261–272, doi:10.1038/s41592-019-0686-2.
[27] J.D. Hunter, Matplotlib: a 2D graphics environment, Comput. Sci. Eng. 9 (3) (2007) 90–95, doi:10.1109/MCSE.2007.55.
[28] V. Kumar, S. Leweke, E. von Lieres, A.S. Rathore, Mechanistic modeling of ion-exchange process chromatography of charge variants of monoclonal antibody products, J. Chromatogr. A 1426 (2015) 140–153, doi:10.1016/j.chroma.2015.11.062.
[29] J.M. Reck, T.M. Pabst, A.K. Hunter, X.Y. Wang, G. Carta, Adsorption equilibrium and kinetics of monomer-dimer monoclonal antibody mixtures on a cation exchange resin, J. Chromatogr. A 1402 (2015) 46–59, doi:10.1016/j.chroma.2015.05.007.
[30] A. Creasy, J. Reck, T. Pabst, A. Hunter, G. Barker, G. Carta, Systematic interpolation method predicts antibody monomer-dimer separation by gradient elution chromatography at high protein loads, Biotechnol. J. 14 (3) (2019) 1800132, doi:10.1002/biot.201800132.
[31] R. Peng, S. Vempala, Solving sparse linear systems faster than matrix multiplication, in: Proceedings of the ACM-SIAM Symposium on Discrete Algorithms (SODA), SIAM, 2021, pp. 504–521, doi:10.48550/arXiv.2007.10254.
[32] G. Strohlein, L. Aumann, M. Mazzotti, M. Morbidelli, A continuous, countercurrent multi-column chromatographic process incorporating modifier gradients for ternary separations, J. Chromatogr. A 1126 (1–2) (2006) 338–346, doi:10.1016/j.chroma.2006.05.011.
[33] A. Püttmann, S. Schnittert, U. Naumann, E. von Lieres, Fast and accurate parameter sensitivities for the general rate model of column liquid chromatography, Comput. Chem. Eng. 56 (2013) 46–57, doi:10.1016/j.compchemeng.2013.04.021.
[34] W.R. Keller, S.T. Evans, G. Ferreira, D. Robbins, S.M. Cramer, Understanding the effects of system differences for parameter estimation and scale-up of high throughput chromatographic data, J. Chromatogr. A 1661 (2022) 462696, doi:10.1016/j.chroma.2021.462696.
[35] T. Hahn, P. Baumann, T. Huuk, V. Heuveline, J. Hubbuch, UV absorption-based inverse modeling of protein chromatography, Eng. Life Sci. 16 (2016) 99–106, doi:10.1002/elsc.201400247.
[36] J.M. Mollerup, A review of the thermodynamics of protein association to ligands, protein adsorption, and adsorption isotherms, Chem. Eng. Technol. 31 (6) (2008) 864–874, doi:10.1002/ceat.200800082.
[37] J. Koch, D. Scheps, M. Gunne, O. Boscheinen, M. Hafner, C. Frech, Mechanistic modeling and simulation of a complex low and high loading elution behavior of a polypeptide in cation exchange chromatography, J. Sep. Sci. 45 (12) (2022) 2008–2023, doi:10.1002/jssc.202200098.
[38] T. Briskot, T. Hahn, T. Huuk, J. Hubbuch, Protein adsorption on ion exchange adsorbers: a comparison of a stoichiometric and non-stoichiometric modeling approach, J. Chromatogr. A 1653 (2021) 462397, doi:10.1016/j.chroma.2021.462397.
[39] J. Diedrich, W. Heymann, S. Leweke, S. Hunt, R. Todd, C. Kunert, W. Johnson, E. von Lieres, Multi-state steric mass action model and case study on complex high loading behavior of mAb on ion exchange tentacle resin, J. Chromatogr. A 1525 (2017) 60–70, doi:10.1016/j.chroma.2017.09.039.
[40] T.C. Huuk, T. Hahn, K. Doninger, J. Griesbach, S. Hepbildikler, J. Hubbuch, Modeling of complex antibody elution behavior under high protein load densities in ion exchange chromatography using an asymmetric activity coefficient, Biotechnol. J. 12 (3) (2017) 1600336, doi:10.1002/biot.201600336.
[41] W. Dai, J. Hahn, J. Kang, Reconstruction of transcription factor profiles from fluorescent protein reporter systems via dynamic optimization and Tikhonov regularization, AIChE J. 60 (11) (2014) 3754–3761, doi:10.1002/aic.14559.